Journal of Materials Chemistry A

Accepted Manuscript

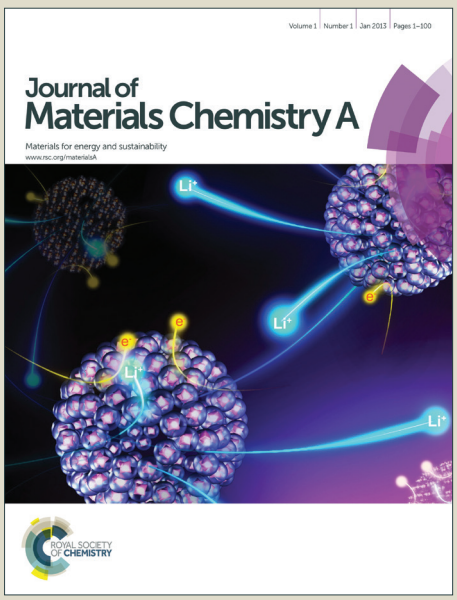

ROYAL SOCIETY OF CHEMISTRY

www.rsc.org/materialsA

Journal of Materials Chemistry A

PAPER

Molten Salt Electrochemical Synthesis of Sodium Titanates as High Performance Anode Materials for Sodium Ion Batteries

Received 00th January 20xx,
Accepted 00th January 20xx

DOI: 10.1039/x0xx00000x

www.rsc.org/

Haomiao Li, Kangli Wang*, Wei Li, Shijie Cheng and Kai Jiang*

Sodium ion batteries are attractive alternatives to lithium ion batteries for stationary energy storage technology, and titanates are considered as promising anode materials for sodium ion batteries. Herein, a series of sodium titanates were synthesized via a simple, fast and controllable electrochemical route from solid TiO_2 in molten salts of NaF-NaCl-NaI. For the first time, the as-prepared $Na_{0.23}TiO_2$ and $Na_{0.46}TiO_2$ were utilized as anode materials for sodium ion batteries, with the sodium storage capacity of 185 m Ah g^{-1} and 215 mA h g^{-1} after 200 cycles, respectively. High rate and long term tests indicated the excellent cycle performance due to the formation of 3D porous electrode structure during the long term charge/discharge processes.

Introduction

Lithium ion batteries (LIBs) are very promising for the application to electrical vehicles in terms of high energy and power density, long cycle life, and relatively mature technology.[1] However, the large consumption of LIBs will drive the increase of price for lithium due to the limited abundance of lithium resources. It's urgent to develop alternative low-cost energy storage technologies for broader market such as large-scale energy storage applications. There is rapidly growing interest on research of sodium ion batteries (SIBs) thanks to the similar physical and chemical properties of sodium with lithium, and the resource abundance and low cost of sodium.[2] However, the larger radius of Na^+ (1.02 Å) compared with Li^+ (0.76 Å) makes Na^+ more difficult for insertion than Li^+. In recent years, more and more attention has been paid to exploring electrode materials to accommodate Na^+. Layered Na_xCoO_2[3], Na_xVO_2[4], $NaNi_{0.5}Mn_{0.5}O_2$[5], $NaNi_{1/3}Mn_{1/3}Co_{1/3}O_2$[6], Na_xFeMnO_2[7] and $NaMPO_4F$ (M= Fe, Mn, V etc.)[8] have been intensively investigated as cathode materials for SIBs. Some vanadium oxide materials[9] and Prussian blue[10] also show potential application for SIBs.

A particular challenge for SIBs is the development of anode material since sodium ion does not intercalate into graphite, which is a popular and low-cost anode material for LIBs. There is no doubt that disordered hard-carbon exhibits the best Na^+ storage properties among the potential carbon candidates. The initial capacities of 300 and 285 mA h g^{-1} for hard carbon were reported by Stevens[11] and Alcántara[12], respectively, but the cyclability was unsatisfactory for the application to SIBs. Ponrouch[13] used hard carbon from sugar pyrolysis as sodium ion batteries anode showed excellent performance with the capacity of 300 mA h g^{-1} at 1/10 C. But the low insertion potential at 0.1 V verves Na electrode may cause safety issue for practical applications. Some metals and alloys, such as Sn[14], Sb[15] and SnSb[16] were regarded as high-capacity anode materials for SIBs. However, the severe problem of large volume change during charge and discharge needs to be further addressed.

Titanium based oxides are promising electrode options for the merits of low toxicity, wide availability and low cost. TiO_2 showed a sodium storage capacity of ~200 mA h g^{-1}.[17] Recently, A. Rudola et al. reported $Na_2Ti_3O_7$ as anode material for SIBs with the average potential of 0.3 V vs. sodium and the insertion of two sodium ions per $Na_2Ti_3O_7$ (177.5 mA h g^{-1}) [18], and Sun et al. reported the capacity of 155 m Ah g^{-1} for spinel $Li_4Ti_5O_{12}$ [19]. The ternary M-Ti-O (M=alkali metal) system consists of various stoichiometric and nonstoichiometric compounds with different applications for energy conversion and storage, such as electro-catalysis and superconductor[20]. The well-known compound is mixed-valence spinel-type $LiTi_2O_4$, with a relatively high Tc (up to 13 K), which has attracted considerable attention following the discovery by Johnston et al. in 1976.[21] The synthesis of M-Ti-O are most through solid reactions of alkali metal or alkali metal compounds with TiO_2 at high temperature(~1000 °C) [22]. For the past few years, Jiang et al. reported an electrochemical route for preparation of Li-Ti-O crystals by electrolysis of a solid TiO_2 cathode in molten slat of LiCl at 700 °C.[23] As facile routes, molten salt based methods are widely used to prepare various functional materials with controlled morphology and tailored physical and electrochemical properties.[24-27]

Herein, for the first time, we reported a simple, fast and controllable synthesis of sires of sodium titanates ($Na_{0.23}TiO_2$, $Na_{0.46}TiO_2$, $NaTi_2O_4$) via electrolysis of solid TiO_2 in molten salts of NaF-NaCl-NaI. The structure and morphology of as-prepared

State Key Laboratory of Advanced Electromagnetic Engineering and Technology, School of Electrical and Electronic Engineering and State Key Laboratory of Materials Processing, and Die & Mould Technology, College of Materials Science and Engineering, Huazhong University of Science and Technology Wuhan, Hubei, China 430074.
E-mail: kjiang@hust.edu.cn; klwang@hust.edu.cn

†Electronic Supplementary Information (ESI) available: [Current-voltage curves of molten salts NaF-NaCl-NaI at 600 °C, and Ex-situ XRD patterns of the $Na_{0.46}TiO_2$@C electrodes]. See DOI: 10.1039/x0xx00000x

sodium titanates were studied and several products were investigated as anode materials of SIBs, which exhibit high performance of Na^+ storage.

Experimental

Preparation of sodium titanates

Electrochemical synthesis. The precursor of TiO_2 powder (EP grade, 0.2-0.4 μm, Aladdin chemistry Co. Ltd.) was ball-milled together with 5 wt.% acetylene black (Kermel Tianjin China) and manually pressed into pellets (diameter, 1.5cm; thickness, ~0.2 cm; weight:, ~1.0 g) with the pressure of ~20 MPa. The addition of acetylene black into TiO_2 pellet is for increasing the conductivity of the pellet in order to accelerate the electrochemical synthesis process. After sintered at 950 °C for 4h under argon atmosphere, the pellets were sandwiched with porous nickel foils and attached onto a clean steel wire. This assembly was used as a cathode with a graphite anode for electrochemical synthesis. The molten salts electrolyte (NaF 15.2%mol-NaCl 31.6%mol-NaI 53.2%mol, melting point: 529.4 °C, all salts from Sinopharm Chemical Reagent Co. Ltd) was stored in graphite crucible and sealed in a stainless retort that was filled with argon.

The electrolysis was conducted at 600 °C with continuous argon flow purging the reactor. Before electrochemical synthesis, pre-electrolysis of the molten salt at 1.8 V was carried out with steel wire cathode and graphite rod anode to remove the residual moisture and some redox-active impurities from the molten salt. The pre-electrolysis usually lasted 2 to 4 hours until the current stabilized at a very small value, which is the so-called background in molten salt electrolysis [28]. The causes for the background current are not fully understood, but are likely attributable to the impurities in salts.[29]

Sodium titanates were synthesized by electrolysis of solid TiO_2 cathode in molten salts at predetermined voltages, which will be further discussed in next section. The electrolysis was terminated after the recorded current decreased to the aforementioned background current value. After electrolysis, the cathode assembly were pulled out from molten salts and cooled in argon, and then washed with deionized water dried at 90 °C overnight for further test.

Cyclic Voltammetry. Cyclic voltammetry was performed to investigate the mechanism of Na^+ insertion into solid TiO_2 in molten salt electrolyte. A "TiO_2 powder modified molybdenum electrode" was used for recording the cyclic voltammograms (CVs) in molten salts (NaF 15.2%mol-NaCl 31.6%mol-NaI 53.2%mol) at 600 °C.[23] The TiO_2 modified electrode was prepared by pressing TiO_2 powder into a fresh and rough end of molybdenum wire, then assembled with a graphite crucible, which contained electrolyte salts and served as counter electrode. The two electrodes and an Ag/AgCl reference electrode were packed into a quartz tube and heated in a resistance furnace. During experiments, argon was continuously purged through the quartz tube. Cyclic voltammetry was performed on the PGSTAT302N potentiostat/galvanostat (AUTOLAB, Netherlands) with potentials ranging from -1.6 to -0.2 V (vs. Ag/AgCl). The Ag/AgCl reference electrode was made by sealing a 0.5 mm diameter Ag wire and 3 wt% of AgCl in NaF-NaCl-NaI eutectic mixture in a closed-end alumina tube (~5 mm diameter, 500 mm length). The end was polished to be a thin microporous layer for conducting ions.

Materials Characterization

The structures and morphologies of as-prepared materials were characterized by X-ray diffraction （XRD）, scanning electron microscopy (SEM) and transmission electron microscopy (TEM). The XRD patterns were obtained on the PANalytical X' Pert PRO (Cu-K generator) in the range of 10-80 degree. SEM analysis was performed with a field-emission scanning electron microscopy (SEM, FEI Nova NanoSEM 450), which electron beam excitation was 5 kV at a beam current of 25 pA. Prior to SEM analysis, samples were gold-sputtered. TEM analysis was performed with a field-emission transmission electron microscopy (TEM, FEI Tecnai G2 F30), which electron beam excitation was 200 kV.

The electrochemical performance of sodium titanates (Na-Ti-O) for anode materials of SIBs was characterized with two-electrode 2016 type coin cells. Among the as-prepared materials, layered structure $Na_{0.23}TiO_2$ and $Na_{0.46}TiO_2$ were tested for coin SIBs. Na-Ti-O powders were dry-ball-milled with 20 wt.% of acetylene black for 24h and formed homologous submicron-composites (Na-Ti-O@C). The Na-Ti-O@C composites were mixed with acetylene black and polyvinylidene fluoride (PVDF) in an 8:1:1 weight ratio. The weight of the materials on individual electrodes was 0.8 ± 0.2 mg cm^{-2} (with 12 mm diameter electrode) and the capacity was reported based on the mass of active materials with conductive agent. N-methyl-pyrrolidone (NMP) was used as a solvent in the mixture to form dense slurry and casted on a copper foil, then dried at 120 °C in vacuum drying oven for 12h. The coin cells were assembled in an Ar filled glove box (O_2 and H_2O < 1 ppm). Sodium disk as the counter electrode, Celgard®2400 (Celgard, LLC Corp., USA) as the separator, and 1 mol/L sodium hexafluorophosphate (NaPF6) in ethylene carbonate (EC) / dimethyl carbonate (DEC) (volume ratio=1:1) as the electrolyte, then performed cyclic voltammetry and galvanostatic cycling by using PGSTAT302N potentiostat/galvanostat (AUTOLAB, Netherlands) and Neware battery tester (Shenzhen, China).

Results and Discussion

Cyclic Voltammertry of Solid TiO_2 in Molten Salts

Figure 1 presents the cyclic voltammograms (CVs) of modified molybdenum electrodes measured in molten NaF-NaCl-NaI at 600 °C. Compared with the electrochemical behavior of blank molybdenum electrode, TiO_2 modified electrode exhibits obvious reduction peaks, which correspond to Na^+ insertion into TiO_2 to form Na_xTiO_2 (0 < x < 1). For the product of reduction peak a' at -1.2 V vs. Ag/AgCl, it will be proven in the next section that the x value is likely to be 0.46. Since the formation of $Na_{0.46}TiO_2$, both electronic and ionic conductivity of cathode increases dramatically and results in the following reduction plateau. Sodium deposition potential in the CV is about -1.6 V (vs. Ag/AgCl). In this work, the decomposition voltage of salts (NaF-NaCl-NaI) is measured to be about 2.5 V at 600 °C (Fig. S1 ESI†). Accordingly, the potential of

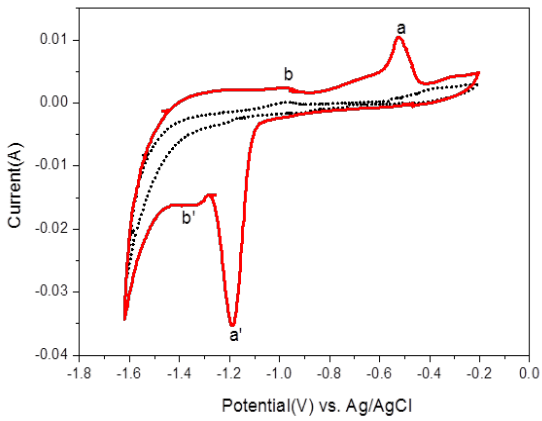

Figure1. Cyclic voltammograms of the molybdenum electrodes modified with (solid line) and without (dashed line) TiO_2 powder in molten NaF - NaCl - NaI at 600 ℃. Scan rate: 0.02 V/s.

-1.2 V vs. Ag/AgCl in three-electrode cell is equivalent to the voltage of about 2.1 V for two-electrode electrolytic cell with graphite anode and modified molybdenum electrode, which determines the voltage for electrochemical synthesis of different titanates.

Physical Characterization of Na-Ti-O Materials

The SEM images of the as-prepared sodium titanates are presented in Figure 2. It can be seen from the images that around hundred-nanometer titanate plates are formed under 1.4 and 2.1 V. The XRD patterns indicate the products at voltage of 1.4 V and 2.1 V are monoclinic $Na_{0.23}TiO_2$ and hexagonal $Na_{0.46}TiO_2$, respectively. The layered structure of $Na_{0.46}TiO_2$ can be further proved by the TEM images in Figure 3. However, the product at voltage of 1.8 V is needle-like $NaTi_2O_4$ with orthorhombic calcium ferrite-type

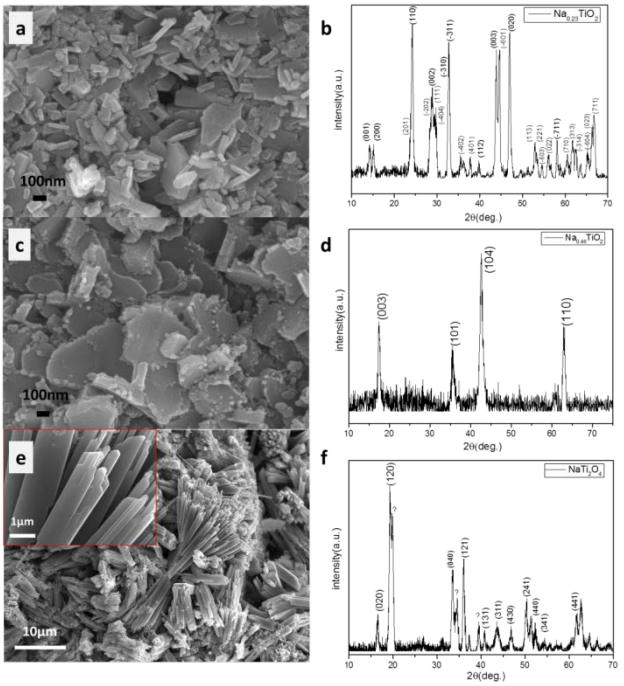

Figure 2. SEM images and XRD patterns of different products synthesized at different voltages: (a) and (b) 1.4 V, (c) and (d) 2.1 V, (e) and (f) 1.8 V.

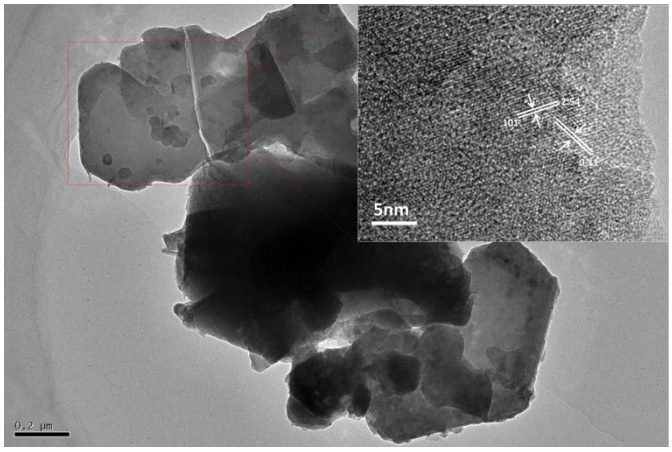

Figure 3. TEM image and HR-TEM image (insert) of $Na_{0.46}TiO_2$ synthesized at voltage of 2.1 V.

structure, which was firstly reported by J. Akimoto and H. Takei in 1989 prepared via solid state synthesis. [30] However, there are several peaks in Figure 2 (f) inconsistent with the structure of $NaTi_2O_4$, which may result from some side-reaction at the voltage of 1.8 V.

Sodium Ion Battery Electrodes Performance Assessment and Analysis

Since there are some impurity phases in $NaTi_2O_4$ product, the studies on SIBs electrode performance of as-prepared sodium titanates are focused on $Na_{0.23}TiO_2$ and $Na_{0.46}TiO_2$. Figure 4 records the cyclic voltammetry (CV) curves of Na_xTiO_2 (x=0.23, 0.46) at a scan rate of 0.2 mV/s within the voltage rang of 0.0-2.5 V versus sodium in 1 mol/L NaPF6 in ethylene carbonate (EC) / dimethyl carbonate (DEC) (volume ratio=1:1) electrolyte. As can be seen in

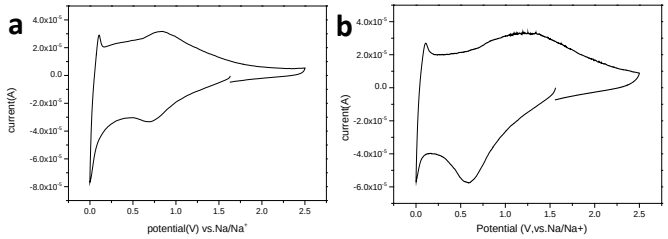

Figure 4. CV curves of the Na_xTiO_2@C composites a) $Na_{0.23}TiO_2$, b) $Na_{0.46}TiO_2$ at a scan rate of 0.2 mV s^{-1}.

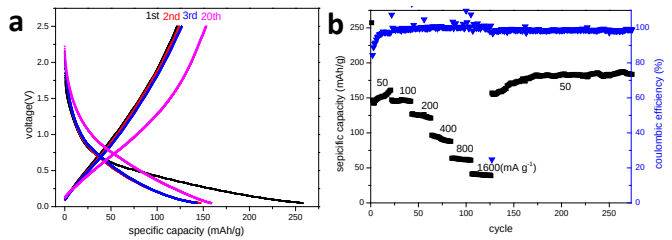

Figure 5. Battery performance of $Na_{0.23}TiO_2$@C composite anode for Na-ion batteries: a) the firstly several charge/discharge curves between 0.05 and 2.5 V at 50 mA g^{-1}. b) Rate performance of $Na_{0.23}TiO_2$ electrode at different discharge current density (50, 100, 200, 400, 800, 1600 mA g^{-1}).

Fig. 4a, there are obvious redox peaks at about 0.7 V and 0.85 V, which could be assigned to the insertion/ extraction of Na^+ into $Na_{0.23}TiO_2$. Very similar to that of $Na_{0.23}TiO_2$, the CV of $Na_{0.46}TiO_2$ exhibits one couple of insertion / extraction peaks. However, it can be noticed that the CV of $Na_{0.46}TiO_2$ exhibits much broader anodic peak, which could be divided into at least two peaks indicating multi-step Na^+ extraction processes. The reaction mechanisms of sodium titanates for sodium ion battery anode are described as following equations:

Discharge: $Na_xTiO_2 + y\ Na^+ \rightarrow Na_{x+y}TiO_2 - y\ e^-$

Charge: $Na_{x+y}TiO_2 - y\ e^- \rightarrow Na_xTiO_2 + y\ Na^+$

(where x = 0.23 or 0.46)

Figure 5a shows the initial several charge/discharge profiles of $Na_{0.23}TiO_2$ composite electrode at a current density of 50 mA g^{-1} between 0.05 V and 2.5 V. The discharge capacity of the first cycle is 257 mA h g^{-1}.The low Coulombic efficiency of the first cycle might be due to the formation of SEI film. [31] It is noteworthy that the capacity increases from ca.150 mA h g^{-1} at the 2nd cycle to 160 mA h g^{-1} at the 20th cycle, and then stabilizes at 185 mA h g^{-1} after 150 cycles. This phenomenon also exists in the case of $Na_{0.46}TiO_2$ electrode material and will be discussed later in this paper. Figure 5b shows the nice rate performance of $Na_{0.23}TiO_2$ with reversible capacity ca. 40 mA h g^{-1} at a high current density of 1.6 A g^{-1}.

$Na_{0.46}TiO_2$ was also tested as anode for SIBs and performed even better than $Na_{0.23}TiO_2$. As shown in Figure 6, at a current density of 50 mA g^{-1}, $Na_{0.46}TiO_2$ delivers a capacity of 323 mA h g^{-1} at the first discharge and ca. 150 mA h g^{-1} discharge capacity for the subsequent several cycles, then stabilizes at ca. 200 mA h g^{-1} after 180 cycles. $Na_{0.46}TiO_2$ also shows high rate and long cycle performance with 120 mA h g^{-1} at 400 mA g^{-1} without obvious fading within 500 cycles.

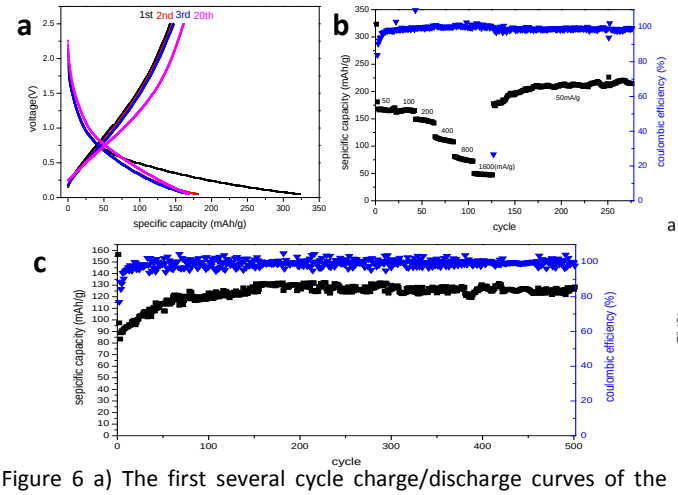

Figure 6 a) The first several cycle charge/discharge curves of the $Na_{0.46}TiO_2$ electrode between 0.05 ~ 2.5 V versus Na electrode at the current density of 50 mA g^{-1}.b) The rate performance of $Na_{0.46}TiO_2$ electrode; c) long-term cycle performance of the electrode at current density of 400 mA g^{-1}

As aforementioned, both $Na_{0.23}TiO_2$ and $Na_{0.46}TiO_2$ exhibit capacity increasing during cycling. To investigate the mechanism of capacity change, the morphologies of electrode before and after cycling were analysed by SEM. As shown in Figure 7, Micrometer and submicrometer particles are adhesive to the copper foil after just one cycle (Figure 7a, 7b). However, the particles turn into smaller size and form a porous structure after 50 cycles, as shown in Fig 7d, which increase the specific surface area of the electrode materials. After 100 cycles, the particles disappear and form 3 dimensional (3D) porous structure (Figure 7e, 7f).The formation of higher surface area and more conductive 3D porous electrode structure results in the capacity increasing, which is in good agreement with the cycling performance showed before. The 3D structure is attributing to the faster transfer of sodium ions and electrons

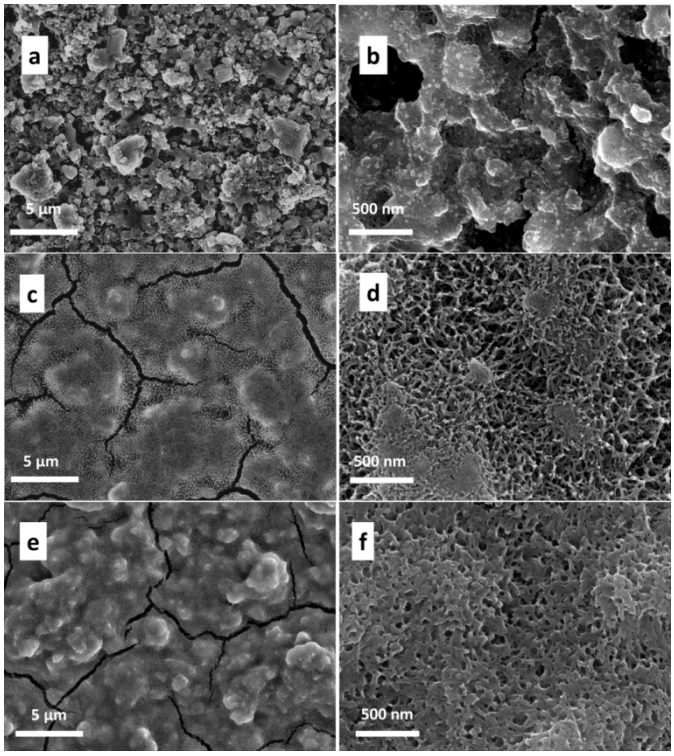

Figure 7. SEM images of $Na_{0.46}TiO_2$ electrode after 1 cycle (a, b), after 50 cycles (c, d), and an electrode after 100 cycles (e, f), respectively.

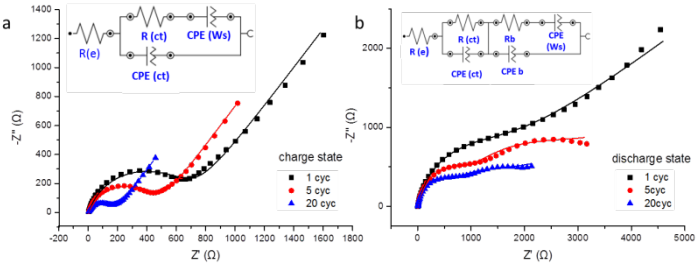

Figure 8. Nyquist plots of the $Na_{0.46}TiO_2$@C electrodes at fully charge state (a) and fully discharge state (b) for various cycle numbers, obtained by applying a sine wave with amplitude of 10 mV in the frequency from 0.1 Hz to 100 kHz. The cells were cycled at 100 mA g^{-1}. Insert figures are the corresponding equivalent electrical circuits for fitting the data.

Table 1 Impedance parameters of $Na_{0.46}TiO_2$@C electrodes at fully charge state and fully discharge state for various cycle numbers

parameter			
Cycle number (charge state)	1	5	20
$R_{(e)}$ (Ω)	3.95	4.10	4.09
$R_{(ct)}$ (Ω)	694	480	196
CPE (μ Mho)	15.4	22.7	83.2
Cycle number (discharge state)	1	5	20
$R_{(e)}$ (Ω)	3.44	2.10	3.40
$R_{(ct)}$ (Ω)	751	626	556
CPE (μ Mho)	6.56	8.22	9.47

during charging/discharging, which also are proved by the electrochemical impedance spectroscopy (EIS) shown in figure 8. The decreasing trends of the electrochemical resistances along with cycle numbers in table 1 reveal the effects from the formation of higher surface area and more conductive 3D porous electrode structure during cycling. Ex-stiu XRD for corresponding electrodes were tested and no structure transformation can be seen for the electrode materials during cycling (Fig. S2 ESI†). This phenomenon may result from the relatively large particles from molten salt method turning into smaller size during charging and discharging, [32] which is similar with the activation process during cycling for some other titanium based electrode materials .[33]

Conclusions

In summary, sodium titanates ($Na_{0.23}TiO_2$, $Na_{0.46}TiO_2$ and $NaTi_2O_4$) were synthesized via a simple and controllable electrochemical route from solid TiO_2 in molten salts of NaF-NaCl-NaI. The synthesis mechanism of sodium titanates and the as-prepared products were systematically characterized by SEM, XRD, CV and galvanostatic cycling. Both single phase $Na_{0.23}TiO_2$ and $Na_{0.46}TiO_2$ delivered stable reversible capacity of 185 mA h g^{-1} and 213 mA h g^{-1} of sodium storage capacity for SIBs, respectively. The as-prepared sodium titanates showed excellent cycling performance and no obvious capacity fading after 500 cycles, which was ascribed to the formation of 3D porous structure during the cycling. This work provides new perspectives for facile electrochemical synthesis of transition metal oxide composites for low-cost and high performance SIBs.

Acknowledgements

This work was supported by the Natural Science Foundation of China (Grant 51307069), the National Basic Research Program of China (973 Program) (2015CB258400) and the National Thousand Talents Program of China.

Notes and references

1 J. B. Goodenough, and K. S. Park, *J. Am. Chem. Soc.*, 2013, 135 (4), 1167–1176.
2 N. Yabuuchi, K. Kubota, M. Dahbi, and S. Komaba, *Chem. Revi.*, 2014, 114(23), 11636-11682.
3 M. D'Arienzo, R. Ruffo, R. Scotti, F. Morazzoni, C. Maria and S. Polizzi, *Phys. Chem. Chem. Phys.*, 2012, 14, 5945–5952.
4 a), D. Hamani, M. Ati, J.M. Tarascon and P. Rozier, *Electrochem. Commun.* 13 (2011) 938–941. b), M. Guignard, C. Didier, J. Darriet, P. Bordet, E. Elkaïm and C. Delmas, Nat. Mater. 2013, 12, 74.
5 H. Kim, I. Park, D. H. Seo, S. Lee, S. W. Kim, W. J. Kwon, Y. U. Park, C. S. Kim, S. Jeon and K. Kang, *J. Am. Chem. Soc.*2012, 134, 10369−10372.
6 M. Sathiya, K. Hemalatha, K. Ramesha, J.-M. Tarascon and A. S. Prakash, *Chem. Mater.*, 24, 10, 1846-1853.
7 a), N. Yabuuchi, M. Kajiyama, J. Iwatate, H. Nishikawa, S. Hitomi, R. Okuyama, R. Usui, Y. Yamada and S. Komaba, Nature Materials, 2012, 11, 512-517.b), H. Zhu, K. T. Lee, G. T. Hitz, X. Han, Y. Li, J. Wan, S. Lacey, A. W. Cresce, K. Xu, E. Wachsman and L. Hu, *ACS applied materials & interfaces*, 2014, 6, 6, 4242-4247.
8 a), B. L. Ellis, W. R. M. Makahnouk, Y. Makimura, K. Toghill and L. F. Nazar, *Nat. Mater.* 2007, 6, 749-753. b), A. Langrock, Y. Xu, Y. Liu, S. Ehrman, A. Manivannan and C. Wang, *J. Power Sources* 2013, 223, 62-67. c), P. Serras, V. Palomares, A. Go˜ni, I. G. Muro, P. Kubiak, L. Lezama, and T. Rojo, *J. Mater. Chem.*, 2012, 22, 22301-22308.
9 a), S. Tepavcevic, H. Xiong, V. R. Stamenkovic, X. Zuo, M. Balasubramanian, V. B. Prakapenka, C. S. Johnson and T. Rajh, ACS nano, 2012, 6, 1, 530–538. b), D. W. Su, S. X. Dou and G. X. Wang, *J. Mater. Chem. A*, 2014, 2, 29, 11185-11194.
10 Y. Lu, L. Wang, J. Cheng and J. B. Goodenough, *Chem. Commun.*, 2012, 48, 6544–6546.
11 D. A. Stevens and J. R. Dahn, *J. Electrochem. Soc.* 2000, 147, 1271-1273.
12 R. Alcántara, P. Lavela, G. F. Ortiz and J. L. Tirado, *Electrochem. SolidState Lett.* 2005, 8, A222-A225.
13 A. Ponrouch, A.R. Goñi, M. Rosa Palacín, *Electrochem. Commun.*, 2013, 27, 85–88.
14 Y. Xu, Y. Zhu, Y. Liu and C. Wang, *Adv. Energy Mater.* 2013, 3, 128–133.
15 J. Qian, Y. Chen, L. Wu, Y. Cao, X. Ai and H. Yang, *Chem. Commun.*, 2012,48, 7070-7072.
16 L. Xiao, Y. Cao, J. Xiao, W. Wang, L. Kovarik, Z. Nie and J. Liu, *Chem. Commun.*,2012, 48, 3321-3323.
17 H. Xiong , M. D. Slater, M. Balasubramanian, C. S. Johnson and T. Rajh, *J. Phys. Chem. Lett.* 2011, 2, 2560-2565.
18 a) A. Rudola, K. Saravanan, C. W. Mason, P. Balaya, *J. Mater. Chem. A*, 2013, 1, 2653-2662; b) H. Pan, X. Lu, X. Yu, Y.-S. Hu, H. Li, X.-Q. Yang and L. Chen, *Adv. Energy Mater.*, 2013, 3: 1186–1194.
19 Y. Sun, L. Zhao, H. L. Pan, X. Lu, L. Gu, Y. -S. Hu , H. Li, M. Armand, Y. Ikuhara, L. Q. Chen and X. J. Huang, *Nat. Commun.*, 2013, 4, 1870, 1-10.
20 M. J. Geselbrachta, A. S. Erickson, M. P. Rogge, J. E. Greedan, R. I. Walton, M. W. Stoltzfus, H. W. Eng and P. M. Woodward, *J. Solid State Chem.*, 2006, 179, 3489–3499.
21 D. C. Johnston, *J. Low Temp. Phys.* 1976, 25, 145–175.
22 a), J. Akimoto and H. Takei, *J. Solid State Chem.*, 1990, 85, 31-37. b), D. Wu, X. Li, B. Xu, N. Twu, L. Liu, and G. Ceder, *Energy Environ. Sci.*, 2015, 8, 195–202.
23 K. Jiang, X. Hu, H. Sun, D. Wang, X. Jin, Y. Ren and G. Z. Chen, *Chem. Mater.*, 2004, 16, 22, 4324-4329.
24 X. Zhao, M. V. Reddy, H. Liu, S. Ramakrishna, G. V. S. Raob and B. V. R. Chowdari, *RSC Advances*, 2012, 2, 7462–7469.
25 M. V. Reddy, B. Zhang, K. P. Loh and B. V. R. Chowdaria, *CrystEngComm*, 2013, 15, 3568-3574.
26 M. V. Reddy, N. Sharma, S. Adams, R. P. Rao, V. K. Peterson and B. V. R. Chowdari, *RSC Advances*, 2015, 5, 29535-29544.
27 M. V. Reddy, C. Y. Quan, K. W. Teo, L. J. Ho and B. V. R. Chowdari, *J. Phys. Chem. C*, 2015, 119, 4709−4718.

28 G. Z. Chen and D. J. Fray, *J. Appl. Electrochem.*, 2001, 31, 2, 155-164.
29 U. Stohr and W. Freyland, *Phys. Chem. Chem. Phys.* 1999, 1, 4383-4387.
30 J. Akimoto and H. Takei, *J. Solid State Chem.* 1989, 79, 212–217.
31 Z. Yan, L. Liu, H. Shu, X. Yang, H. Wang, J. Tan, Q. Zhou, Z. Huang, X. Wang, *J. Power Sources*, 2015, 274, 8-14.
32 Y. Kim, Y. Kim, Y. Park, Y. N. Jo, Y. Kim, N. Choia and K. T. Lee, *Chem. Commun.* 2015, 51, 50-53.
33 H. Xiong, M. D. Slater, M. Balasubramanian, C. S. Johnson, and T. Rajh, *J. Phys. Chem. Lett.*, 2011, 2, 2560–2565.

ToC

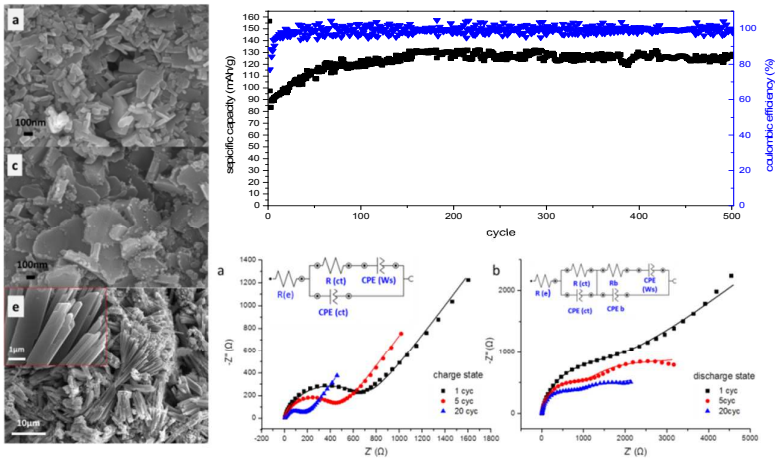

Sodium titanates are synthesized via a facile molten salt based electrochemical route and exhibit high performance of Na^+ storage.